1.1 A/mm β-Ga_2O_3-on-SiC RF MOSFETs with 2.3 W/mm P_{out} and 30% PAE at 2 GHz and f_T/f_{max} of 27.6/57 GHz

Min Zhou[1], Hong Zhou[1*], Sen Huang[2], Mengwei Si[3], Yuhao Zhang[4], Tiantian Luan[2], Hongqing Yue[1], Kui Dang[1], Chenlu Wang[1], Zhihong Liu[1], Jincheng Zhang[1*], and Yue Hao[1]

[1]Key Laboratory of Wide Band Gap Semiconductor Materials and Devices, School of Microelectronics and Guangzhou institute of technology, Xidian University, Xi'an 710071, China, *email: hongzhou@xidian.edu.cn, jchzhang@xidian.edu.cn

[2]Institute of Microelectronics of Chinese Academy of Sciences, Beijing 100029, China

[3]Department of Electronic Engineering, Shanghai Jiao Tong University, Shanghai 200240, China

[4]Center for Power Electronics Systems, Virginia Polytechnic Institute and State University, Blacksburg 24060, USA

2023 International Electron Devices Meeting (IEDM) | 979-8-3503-2767-0/23/$31.00 ©2023 IEEE | DOI: 10.1109/IEDM45741.2023.10413782

Abstract**—**This work demonstrates for the first time the power performance of β-Ga_2O_3 RF transistors at 2-8 GHz with a record high output power density (P_{out}) of 2.3 W/mm and a power-added efficiency (PAE) of 30% at 2 GHz. Such P_{out} and PAE are 25 and 3 times of previous state-of-the-art β-Ga_2O_3 RF power devices at 2 GHz, respectively. In addition, the device shows a maximum on-current ($I_{D,max}$) of 1.1 A/mm and a f_T/f_{max} of 27.6/57 GHz, all among the highest in β-Ga_2O_3 RF devices. Such RF performances are enabled by transferring a heavily-doped β-Ga_2O_3 channel to a SiC substrate, which significantly reduce the on-resistance and improve the heat dissipation, as well as deploying an insulated and recessed T-gate to simultaneously enhance the frequency performance and electric field management. These results indicate a remarkable progress in the field of β-Ga_2O_3 RF power devices and show the promise of β-Ga_2O_3-on-SiC platform for high-power, high-frequency, high-efficiency RF applications.

I. Introduction

Ultra-wide bandgap semiconductor β-Ga_2O_3 has gained increased attentions for RF and power electronics applications, arising from its 4.6-4.8 eV bandgap induced high critical field (E_c) of ~8 MV/cm, low-cost and low-defect density material, as well as high saturation velocity (ν_{sat}) of 1.5~2×10^7 cm/s [1]. β-Ga_2O_3 promises a superior Johnson Figure-of-merit (J-FOM) over GaN. Recently, fast advances have been reported on the f_T/f_{max} of β-Ga_2O_3 devices. For example, Saha *et al*. reported a f_T/f_{max} of 11/48 GHz and $I_{D,max}$ of 285 mA/mm in a β-Ga_2O_3 MOSFET [2], and the authors reported an enhanced f_T/f_{max} of 27/100 GHz and $I_{D,max}$=160 mA/mm in their latest pre-print [3].

Despite the progress on f_T/f_{max}, the RF power performance of β-Ga_2O_3 devices is still limited. The state-of-the-art β-Ga_2O_3 RF transistors only achieved a P_{out}/PAE of 0.45 W/mm/10% at 1 GHz and a P_{out}/PAE of 0.08 W/mm/9% at 2 GHz [4]-[9]. This is mainly due to the very low thermal conductivity (k_T) of β-Ga_2O_3 and the relative low channel doping usually used in RF devices, which make it very difficult to achieve efficient heat dissipation and high $I_{D,max}$. The limited RF power has become a key roadblock that needs to overcome to take full advantage of the high E_c and ν_{sat} of β-Ga_2O_3 in RF power devices.

This work addresses this challenge by demonstrating over 25X higher P_{out} (2.3 W/mm) and 3X PAE (30%) at 2 GHz in a β-Ga_2O_3 RF MOSFET, as well as an expanded signal amplification range up to 8 GHz with P_{out} near 1 W/mm. The devices also shows a $I_{D,max}$ of 1.1 A/mm, which is the highest reported in β-Ga_2O_3 RF transistors, as well as a f_T/f_{max} of 27.6/57 GHz. The key to achieve such performance is the innovative combinations of several device designs: 1) β-Ga_2O_3 thin layer is transferred to a high-k_T SiC substrate to boost the heat dissipation, 2) a heavily-doped β-Ga_2O_3 channel layer is adopted with the optimized Ohmic contact to reduce the device on-resistance (R_{ON}) and upscale $I_{D,max}$, 3) an insulated, recessed T-gate is used to improve high f_T/f_{max}, at the same time forming a field plate for electric field management, which allows the device to achieve a breakdown voltage (BV) of 150 V across a short gate-to-drain distance (L_{GD}) of 0.7 μm.

II. Experiments

Fig. 1 shows the 3-D device schematic of β-Ga_2O_3 RF power FETs. A heavily Sn-doped (3×10^{18} cm^{-3}) channel layer was transferred from (-201) bulk substrate to a SiC substrate, which is similar to the ion-cutting and exfoliating processes as reported in Ref. [10]. After that, CMP was used to planarize the surface, followed by BCl_3 dry etching to thin down the channel layer from ~500 nm to 100-110 nm. The full process, including the mesa isolation, ion implantation, Ohmic formation, gate recess, ALD Al_2O_3, T-gate formation, and surface passivation, is illustrated in **Fig. 2**. Si implantation with a dose of ~10^{15} cm^{-2} was used to lower the contact resistance (R_c). After the transfer process and gate recess etch, a Piranha clean was adopted to reduce the surface defect. **Fig. 3** shows the AFM image of the β-Ga_2O_3 surface after dry etch and Piranha clean, revealing an RMS roughness of only 0.25 nm. **Fig. 4** shows the top view and cross-sectional SEM images of the dual-gate MOSFETs. Devices have a gate length (L_G) of 180 nm, gate width (W_G) of 2×30 μm and 2×25 μm, source-drain distance (L_{SD}) of 1.3 μm, and L_{GD} of 0.7 μm. Gate recess depth of 45 nm is implemented to improve gate control and reduce the short channel effect. The TLM measurements reveals a low R_c of 0.55 Ω·mm (**Fig. 5**).

III. Results and Discussion

Well-behaved output characteristics (I_D-V_{DS}) of the β-Ga_2O_3 RF power FET are shown in **Fig. 6(a)** with V_{GS} stepped from 8 V to -20 V and V_{DS} swept from 0 V to 15 V. The R_{on} and $I_{D,max}$ are extracted to be 10 Ω·mm and 1.1 A/mm, respectively. Log-scale transfer characteristics (I_D-V_{GS}) are exhibited as **Fig. 6(b)** with V_{DS} stepped from 1 V to 15 V. A

SS=160 mV/dec, on/off ratio of 10^8, and I_G<10^{-8} A/mm are achieved. Linear-scale I_D-V_{GS}-g_m characteristics are displayed in **Fig. 7**, where threshold voltage V_T=-13 V and $g_{m,max}$ = 70 mS/mm are extracted. Since β-Ga_2O_3 material has a decent μ, high E_c, and high ν_{sat}, a higher V_{DS} can be accessed to allow a higher field to accelerate electrons and reach ν_{sat}. **Fig. 8** shows the I_D-V_{DS} characteristics with max V_{DS} = 10 V to 25 V in the sweep; the device can operate at V_{DS} of 25 V at V_{GS} of 4 V.

Fig. 9 depicts the pulse measurement results of the β-Ga_2O_3 RF MOSFETs at various quiescent bias points (V_{GSQ}, V_{DSQ}), namely cold channel (0 V, 0 V), gate pulse (-20 V, 0 V) and drain pulse (-20 V, 25 V) at a pulse period of 50 μs, width of 5 ms and V_{GS} = 6 V. Compared with the DC curve, all the pulsed $I_{D,max}$ are only slightly higher (3.5%) even at a high V_{DS} = 20 V, verifying the suppression of the self-heating effect. In addition, compared with cold channel state, the gate and drain pulsed $I_{D,max}$ shows no obvious change (< 2%). The lack of current collapse verifies the high quality MOS and β-Ga_2O_3 materials, which is key to achieve high P_{out} and PAE at high V_{DS}.

Fig. 10(a) shows the 3-terminal off-state breakdown results of the device at V_{GS} = -25 V. Even with a high doping concentration of 3×10^{18} cm^{-3} and small L_{GD} = 0.7 μm, the BV reaches 150 V, translating to an average E-field of 2.15 MV/cm. This is believed to be due to the field plate formed by the T-gate. As shown in the simulated E-field contour in **Fig. 10(b)**, the field plate suppresses the peak E-field at the gate edge. The extracted peak E-field in the β-Ga_2O_3 channel and SiC substrate are 8 MV/cm and 3 MV/cm, respectively, suggesting a full exploitation of the high E_c of WBG and UWBG materials.

Small-signal RF characterization of one representative RF MOSFET is carried out at peak g_m condition and V_{DS}=20 V, as shown in **Fig. 11**. The off-wafer standard LRRM calibration and on-wafer open structure are used to calibrate the network analyzer and de-embed pad parasitic, respectively. The f_T is given by linear extrapolation of the H_{21} gain with a conservative slope of -20 dB/dec at low f regions, yielding a f_T=27.6 GHz. The f_{max} is determined by a similar way with a -20 dB/dec slope from G_u or MAG/MSG, yielding a f_{max} = 57 GHz. The $f_T\times L_G$ is yielded to be ~5 GHz·μm and the $(f_T\times f_{max})^{0.5}$ is determined to be 39.7 GHz. V_{GS} and V_{DS} dependent f_T/f_{max} mapping are displayed in **Fig. 12(a)** and **12(b)**. It is evident that f_T and f_{max} are maximized at V_{GS} with peak g_m. The higher V_{DS} increases the E-field along the channel so that the velocity is higher and hence the f_T/f_{max} is increased at higher V_{DS}. It is beneficial for power amplifiers to operate at higher V_{DS} to maximize the gain.

Large-signal load-pull characterizations of the same device when biased at class-AB with input and output matched are shown in **Fig. 13(a)** at a f=2 GHz, V_{DS}=25 V and 35 V. The input signal is under **continuous wave** mode and maximum V_{DS} = 35 V is limited by our equipment. Maximum P_{out} = 2.3 W/mm and PAE = 31% are achieved. V_{DS} dependent P_{out} and PAE are depicted in **Fig. 13(b)** with a P_{out} increment of ~0.5 W/mm per 5 V V_{DS} increase. Considering BV = 150 V, the P_{out} of this RF MOSFET is estimated to be 7 W/mm at a V_{DS}= 80 V. Continuous wave 3 GHz, 5 GHz and 8 GHz load-pull measurements at V_{DS} = 25 V are presented as **Fig. 14**, **Fig. 15(a)** and **Fig 15(b)**. The extracted P_{out}/PAE at three frequencies are 1.5 W/mm/25%, 1.3 W/mm/17%, and 0.7 W/mm/7%, respectively. To date, this is the first demonstration of an oxide semiconductor RF power FET that amplifies signal up to 8 GHz.

IV. Benchmarking and Conclusions

Fig. 16 benchmarks the I_{Dmax} *vs.* $g_{m,max}$ of our β-Ga_2O_3-on-SiC RF MOSFET with the state-of-the-art top-gate β-Ga_2O_3 RF transistors, including MOSFETs and HFETs with delta-doping. Our device shows the highest $I_{D,max}$ and $g_{m,max}$, and $I_{D,max}$ nearly doubles the prior highest value. These record DC performances set a basic foundation for β-Ga_2O_3 RF FET to minimize the R_{on} related delay and obtain a high f_T/f_{max}. **Fig. 17(a)** summarizes the f_{max} *vs.* $f_T\times L_G$ behavior of our FETs when compared with other representative oxide transistors, including ITO [11], In_2O_3 [12] and Ga_2O_3. The $f_T\times L_G$ = 5 GHz·μm and f_{max}=57 GHz are among the highest values in all the peer-review published reports (the results in pre-print [3] are not included for now).

The large-signal performance of our device is benchmarked against other best β-Ga_2O_3 transistors in the plot of P_{out}~PAE in **Fig. 17(b)** [5]-[9]. Our device increased the P_{out} for over 25 times while maintaining a record PAE=30% at f=2 GHz, as well as expanded the signal amplification range from 2 GHz to 8 GHz with P_{out}~1 W/mm. This advance is in part attributable to the β-Ga_2O_3-on-SiC platform, which enables the significantly improved heat dissipation as compared to prior β-Ga_2O_3 RF power transistors which are all fabricated on β-Ga_2O_3 substrate.

In conclusion, for the first time we have expanded the signal amplification range of β-Ga_2O_3 RF power devices from 2 GHz to 8 GHz. Our device innovatively combines the β-Ga_2O_3-on-SiC material platform, highly-doped β-Ga_2O_3 channel, and a T-gate with field plate, which allows for a concurrent realization of the efficient heat extraction, low R_{ON}, high $I_{D,max}$, high BV, and high f_T/f_{max}. The demonstrated device performances include $I_{D,max}$ = 1.1 A/mm, f_{max} = 57 GHz, CW P_{out}/PAE= 2.3 W/mm/30%@2 GHz, 1.5 W/mm/25%@3 GHz, 1.3 W/mm/17%@5 GHz and 0.7 W/mm/7%@8 GHz, setting several new records in β-Ga_2O_3 RF power transistors. These results also show the great promise of β-Ga_2O_3-on-SiC RF FETs for future high-frequency, high-power, and high-efficiency applications.

Acknowledgment

The authors gratefully acknowledge the funding support in part from NSFC with grant nos. of 62222407 and 62004147, and in part from Guangdong Provincial NSF under the grant no. of 2023B1515040024.

References

[1] M. Higashiwaki et al., *Appl. Phys. Lett.,* vol. 100, no. 1, 2012.
[2] C. N. Saha et al., *Appl. Phys. Lett.,* vol. 122, p. 182106, 2023.
[3] C. N. Saha et al., arXiv:2305.04725, 2023.
[4] A. J. Green et al., *IEEE Electron Device Lett.*, vol. 38, p. 790, 2017.
[5] K. D. Chabak et al., *in 2018 IEEE IWMS-AMP*, p. 13.
[6] M. Singh, et al., *IEEE Electron Device Lett.*, vol. 39, p. 1572, 2018.
[7] Z. Xia et al., *IEEE Electron Device Lett.*, vol. 40, p. 1052, 2019.
[8] N. A. Moser., *IEEE Electron Device Lett.*, vol. 41, p. 989, 2020.
[9] X. Yu et al., *IEEE Electron Device Lett.*, vol. 44, p. 1060, 2023.
[10] W. Xu et al., *in 2019 IEEE Int. Electron Devices Meet.*, pp. 5.4.
[11] Q. Hu et al., Science Adv., vol. 8, p. eade407, 2022.
[12] D. Zheng et al., in 2023 Symp. VLSI Tech.

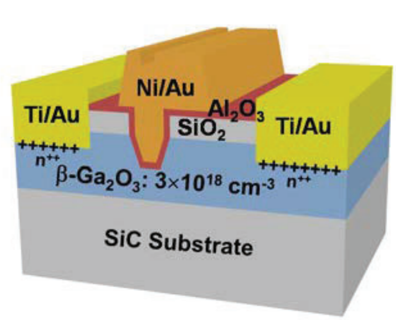

Fig. 1: 3D cross-sectional schematic view of β-Ga_2O_3 RF power FET on a SiC substrate. Heavily doped channel is used to reduce R_{on} and a gate recess structure is used to enhance the gate control and frequency performance.

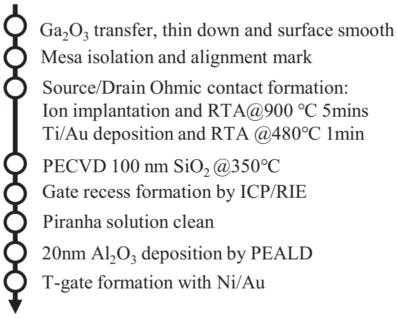

Fig. 2: Key fabrication process steps of β-Ga_2O_3 RF power FETs, including β-Ga_2O_3 transfer and layer thinning, Ohmic contact, piranha clean, ALD dielectric deposition and passivation, and gate contact formation.

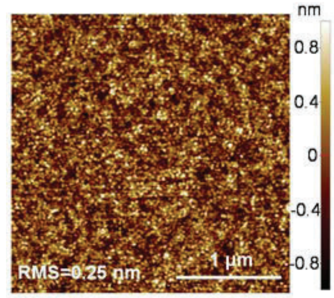

Fig. 3: Atomic force microscopy (AFM) image of the piranha solution treated β-Ga_2O_3 thin film. After CMP, dry etch, and piranha clean, the RMS roughness is 0.25 nm.

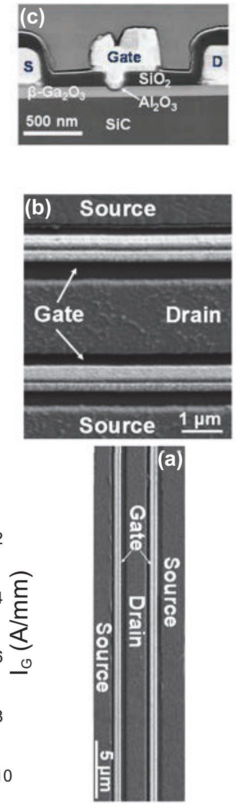

Fig. 4: (a) Top view, (b) zoomed-in view, (c) cross-sectional view of β-Ga_2O_3 RF power FETs with L_G=180 nm, recess depth of 45 nm, and a β-Ga_2O_3 total thickness of 100 nm.

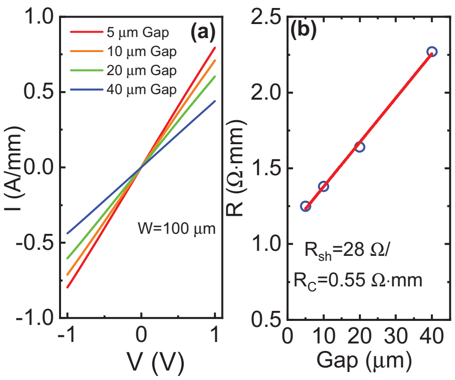

Fig. 5: (a) I-V curves of various TLM spacing pads after ion implantation. (b) R_c and R_{sh} extraction through linear extrapolation with R_c = 0.55 Ω·mm and R_{sh} = 28 Ω/□.

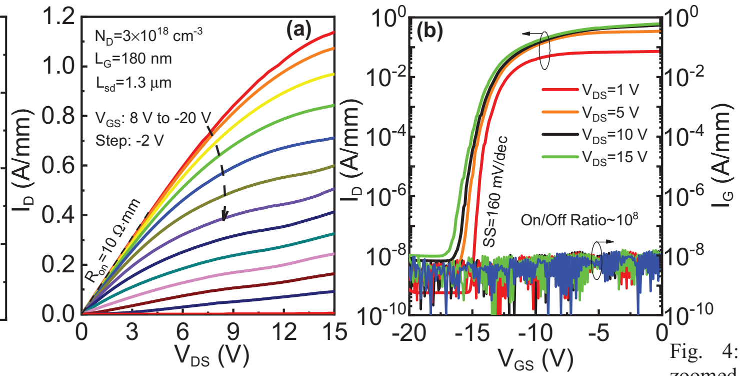

Fig. 6: Well-behaved (a) linear-scale I_D-V_{DS} and (b) log-scale I_D-V_{GS}-I_G characteristics of representative β-Ga_2O_3 RF power FET with L_G = 180 nm and $N_D=3\times10^{18}$ cm^{-3}. Record $I_{D,max}$ = 1.1 A/mm and high on/off ratio of 10^8 are achieved.

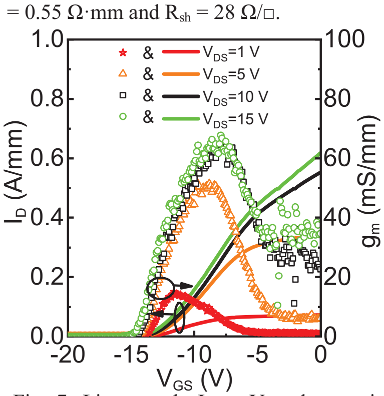

Fig. 7: Linear-scale I_D-g_m-V_{GS} characteristics of the device as Fig. 6. The V_T is extracted to be -13 V and the $g_{m,max}$ is 70 mS/mm, which is one of the highest values reported in β-Ga_2O_3 RF FETs.

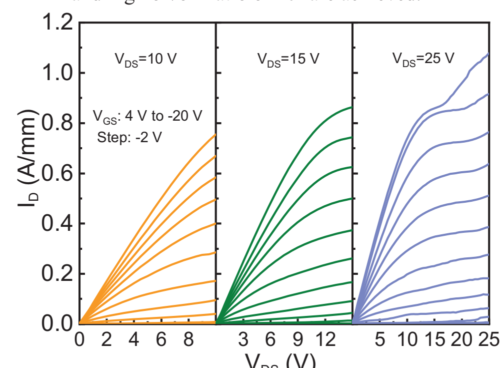

Fig. 8: V_{DS} dependent I_D-V_{DS} characteristics of the same device to evaluate the impact of max V_{DS} to the I_D. Before the device burn-out, a maximum V_{DS}=25 V is applicable even at a V_{GS} = 4 V.

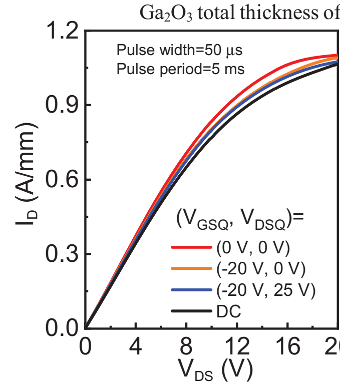

Fig. 9: Pulsed $I_D - V_{DS}$ characteristics of the same device with 50 μs pulse width and 1% duty cycle. Gate pulsed and drain pulsed $I_{D,max}$ are similar to the cold channel and DC $I_{D,max}$, verifying the suppressed self-heating and current-collapse effect, as well as the high quality of the oxide/ semiconductor interfaces and the transferred β-Ga_2O_3 channel layer.

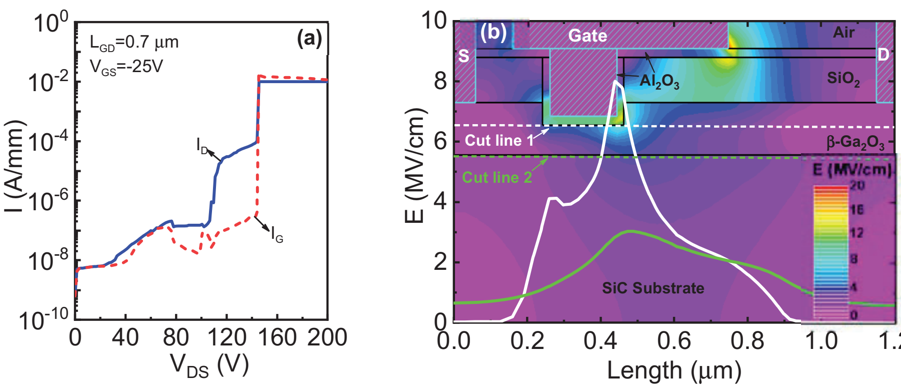

Fig. 10: (a) Three-terminal off-state breakdown characterization of the device with L_{GD}=0.7 μm at a V_{GS}=-25 V. (b) TCAD Simulation of the E-field contour of the same device at a BV =150 V and V_{GS}=-25 V. Even with a $N_D=3\times10^{18}$ cm^{-3} and small L_{GD} =0.7 μm, a BV=150 V and an averaged E>2 MV/cm are achieved, showing that heavily doped β-Ga_2O_3 RF FET can be used as high voltage power amplifier to enhance the P_{out}.

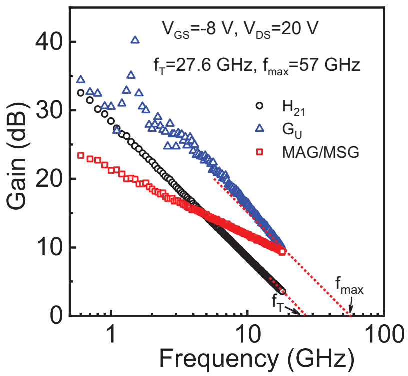

Fig. 11: Small-signal RF performance of a Ga_2O_3 RF FET with L_G = 180 nm when biased at V_{GS} = -8 V and V_{DS} = 20 V. f_T/f_{max}= 27.6/57 GHz are extracted.

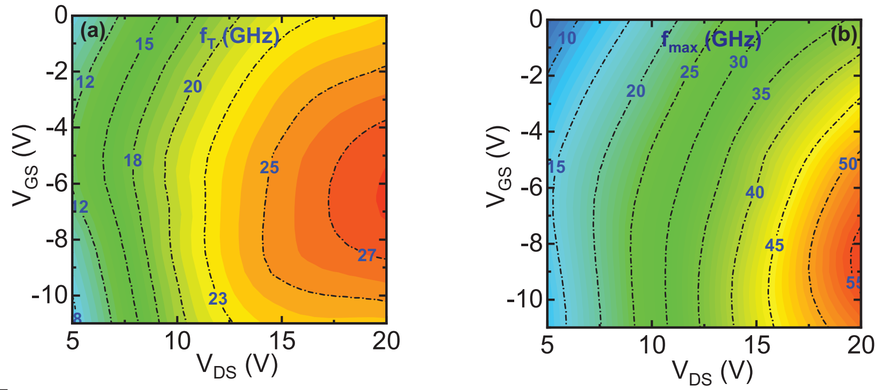

Fig. 12: Extracted (a) f_T and (b) f_{max} dependence on the V_{GS} and V_{DS} mapping contour. Peak f_T and f_{max} occurs at peak g_m corresponded V_{GS} point. f_T and f_{max} increase along with the increase of V_{DS}, indicating a higher V_{DS} can induce higher E-field to get a higher velocity for a higher frequency.

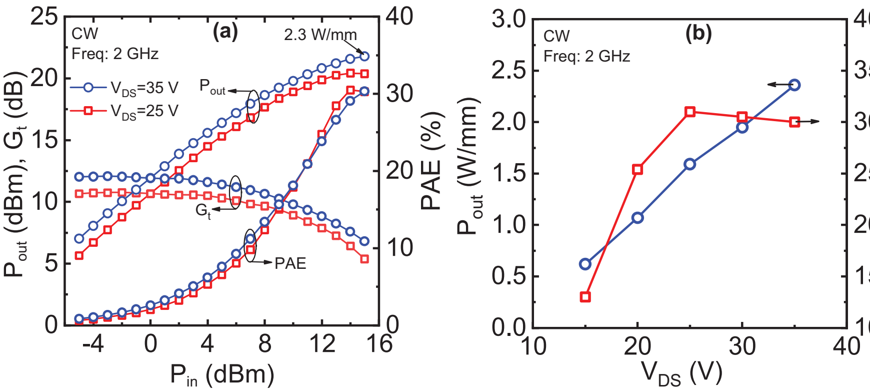

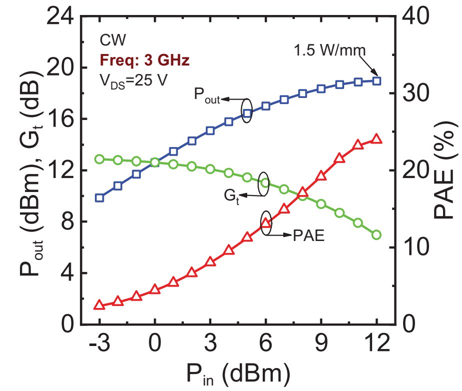

Fig. 13: (a) Continuous wave (CW) large-signal class-AB performance of the device with power sweep at f=2 GHz and V_{DS} = 25/35 V. (b) P_{out} and PAE dependence on the V_{DS} from 15 V to 35 V with 5 V as a step. Record P_{out} = 2.3 W/mm and PAE=31% are achieved. The device is with W_G=2×30 μm.

Fig. 14: CW f=3 GHz large-signal performance of the device with W_G=2×25 μm at a V_{DS} = 25 V. P_{out}/PAE = 1.5 W/mm/25% are simultaneously demonstrated.

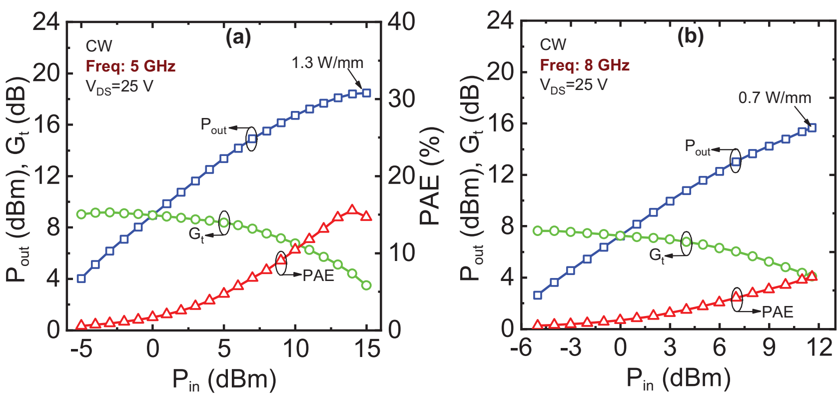

Fig. 15: CW (a) f=5 GHz and (b) 8 GHz large-signal performance of the same device as Fig. 14 at a V_{DS} = 25 V. P_{out}/PAE = 1.3 W/mm/17% and 0.7 W/mm/7% are achieved for f=5 GHz and 8 GHz, respectively. Our device sets a new record for the power performance of β-Ga_2O_3 RF FETs.

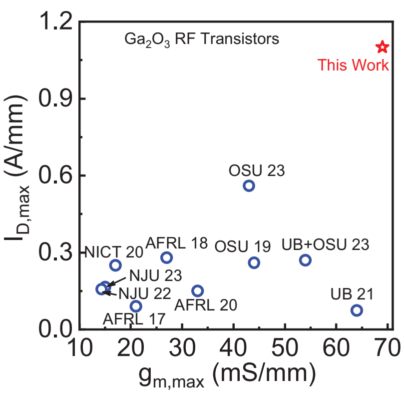

Fig. 16: $I_{D,max}$ versus $g_{m,max}$ benchmark plot comparison of our β-Ga_2O_3-on-SiC RF power FETs with other β-Ga_2O_3 RF FETs. By implementing a heavily doped channel and high thermal conductivity SiC substrate, the $I_{D,max}$ is twice of previous record $I_{D,max}$ value.

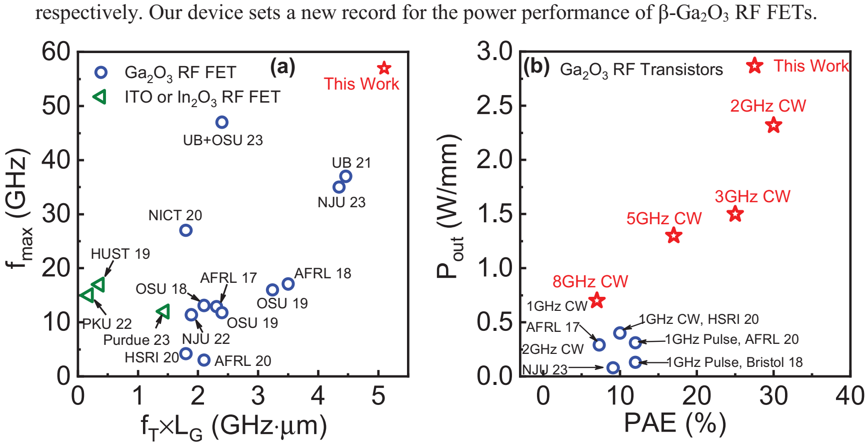

Fig. 17: (a) f_{max} versus f_T×L_G and (b) P_{out} versus PAE benchmark of our β-Ga_2O_3-on-SiC RF power FETs with other β-Ga_2O_3 RF FETs. Benefited from the record $I_{D,max}$ and $g_{m,max}$, our f_{max}=57 GHz is among the highest among all oxide RF FETs. By combining the suppressed self-heating and current-collapse effects, CW P_{out}/PAE = 2.3 W/mm/30%@f = 2 GHz are the highest value among all the reported results, and the P_{out} is over 25 times higher than previous record P_{out}@f=2 GHz. In addition, we first report the large-signal performance of β-Ga_2O_3 RF power FETs from f = 3 GHz to f = 8 GHz. P_{OUT}/PAE = 1.5 W/mm/25%@3 GHz, 1.3 W/mm/17% @5 GHz, and 0.7 W/mm/7%@8 GHz are a new record for the β-Ga_2O_3 RF power FETs.